A comparison of RCMs and meteorological time series (1950-1996) of southern Italy as a fine calibration for hydrogeological scenarios

Daniele Lepore[1], Edoardo Bucchignani[2], Myriam Montesarchio[2], Vincenzo Allocca[1], Delia Cusano[1] & Pantaleone De Vita[1]

[1] Department of Earth, Environmental and Resource Sciences (DiSTAR), University of Naples Federico II, Naples, 80126, Italy

[2] Meteorology Laboratory, Centro Italiano Ricerche Aerospaziali (CIRA), Capua, 81043, Italy

Correspondence to: Daniele. Lepore (daniele.lepore@unina.it)

Abstract. Nowadays the phenomenon of Global Warming is unequivocal, as confirmed by the latest reports of the IPCC and studies of the climate-change impacts on ecosystems, global economy, and populations. Among these analyses the effect of climate change on groundwater is a very relevant task especially for regions whose economic and social development depends chiefly on groundwater availability, as for the southern Italy. In such a territorial framework, this research was focused on analyzing: i) comparison of precipitation and air temperature obtained by Regional Climate Models (RCMs) and meteorological time series recorded in a part (1950-1996) of the "historical experiment" period (1950-2005); ii) effects of climate change on scenarios of air temperature (T) and precipitation (P) and, consequently, on scenarios of actual evapotranspiration (ETR) and effective precipitation Pe (P – ETR). The latter was considered as a proxy of groundwater recharge of the principal aquifer systems of the region, represented chiefly by the karst aquifers.

To achieve a detailed hydro-climatological characterization, an Ensemble of 15 RCMs (E15) derived from the European Coordinated Regional Downscaling Experiment (EURO-CORDEX), at a spatial resolution of 0.11° (~12 km), was analyzed. Specifically, two IPCC Representative Concentration Pathways of greenhouse gases (RCP4.5 and RCP8.5) were considered. The E15 was calibrated in the validation period (1950-1996) by a statistical comparison with data observed by the regional meteorological network managed by the former National Hydrological Service (SIMN), Department of Naples, which was active in the period 1921-1999.

As a principal result, the E15 was found with a statistical structure very similar to those of observed annual precipitation (OBS$_P$) and mean annual air temperature (OBS$_T$), characterized by a very similar frequency distribution. Accordingly, an inferential statistical approach was performed for calibrating E15 precipitation (E15$_P$) and air temperature (E15$_T$) based on the compensation of the difference with OBS$_P$ (+7%) and OBS$_T$ (-16%). The E15 projects a reduction in precipitation and an increase in air temperature under both RCPs, with a divergence point between the two scenarios occurring by about 2040. As a principal result, Pe shows declining trends for both RCP scenarios, reaching a decrease of the 11-yrs moving average down to -20%, for RCP4.5, and -50%, for RCP8.5, even if characterized by relevant inter-annual fluctuations.

1 Introduction

The economic and social development of southern Italy is fundamentally sustained by the availability of groundwater
35 resources which supply the principal aqueduct systems of drinkable water as well as the agriculture and industrial activities.
Moreover, groundwater resources play a fundamental role in nourishing many coastal and continental groundwater-
dependent ecosystems.

The great relevance of groundwater resources of the region is principally due to the occurrence of aquifer systems
characterized by the highest mean annual groundwater yield in Europe, among which karst aquifers are the most significant
40 (Stevanović, 2018).

The strong dependence on groundwater resources makes the socio-economic and environmental settings of southern Italy
very vulnerable to the effects of climate change. Notwithstanding this, the current Italian laws and policies on groundwater
management still lack measures aimed at mitigating risks of groundwater crisis due to the climatic variability. Recent
examples are the hydrologic years 2015-2016, 2016-2017 and 2020-2021, when the amount of precipitation of winter
45 recharge periods were significantly lower than the average values, causing a severe shortage of major spring discharges and
deep concern about scenarios to be expected at the end of the dry season and in the following hydrological years.
Consequently, the analysis of future hydrogeological scenarios appears as a fundamental achievement for a resilient
management of groundwater resources in southern Italy.

Despite the important relationship between climate patterns and groundwater resources (Taylor et al., 2013), researches have
50 not advanced the analysis of the future impacts of climate change on groundwater recharge processes to the same extent of
those carried out on surface water resources (Green et al., 2011). Accordingly, this study aims to analyse the effects of the
climate change on the groundwater recharge processes of the major aquifers systems of the southern Italy, by the application
of data provided by Regional Climate Models (RCMs), which are currently used to project scenarios of atmospheric
variables (e.g. precipitation (P) and air temperature (T)) until the end of the XXI century. RCMs are widely employed by the
55 scientific community due to their high resolution, being able to provide key inputs to studies regarding the impact of climate
change on natural and anthropic systems, thus allowing the planning of adaptation measures by addressing potential damages
and opportunities.

In this work, the estimation of changes in annual values of actual evapotranspiration (ETR) and effective precipitation (Pe)
until 2100 is based on an ensemble of RCMs simulations belonging to the European branch of the CORDEX initiative
60 (Giorgi et al., 2009), being the latter considered as a proxy of groundwater recharge of principal aquifer systems, among
which the karst aquifers are the most relevant in southern Italy.

The remaining of the paper is organized as follows: a literature review of RCMs application in the hydrogeological field on
karst aquifers in the Mediterranean area is presented in Sect. 2, then Data and methods, Results, Discussion and Conclusions
are provided in Sects. 3, 4, 5 and 6, respectively.

65

2 RCMs in the Mediterranean area

General Circulation Models (GCMs) and RCMs are applied worldwide with different spatial resolutions and temporal scales, succeeding to develop climate scenarios up to the end of the current century. A series of international projects and studies
70 (e.g. CORDEX) (Giorgi et al., 2009) have produced a huge ensemble of climate projections, accounting for most of the uncertainties affecting climate change predictions (Fernández et al., 2019). Holman (2012) suggested that the best practice for using climate model projections to assess the impact on groundwater resources was to consider multiple GCMs or RCMs under different emission scenarios (pathways). This approach introduces additional variability in the climate data, which enhances uncertainty in the assessment of future groundwater recharge (Kurylyk & MacQuarrie, 2013).

75 To verify the state of the art of the application of climate models, both GCMs and RCMs were considered in the framework of Mediterranean karst aquifers for assessing: i) methodology and variables used to generate potential future climate scenarios; ii) spatial and temporal resolution of the models; iii) applications of GCMs and RCMs to assess groundwater recharge; iv) groundwater recharge methods. A summary of the state of art is shown in Table 1.

The studies focused on the application of GCMs and RCMs in Mediterranean areas were based on various combinations of
80 the models to increase the reliability of the predicted future scenarios and reduce their uncertainty with specific approaches for bias correction. Most of the RCMs applied derive from the EURO-CORDEX project (Jacob et al., 2014). The EURO-CORDEX team performed a dynamical downscaling of the global simulations from the CMIP5 long-term experiments. They are based on greenhouse gas scenarios (Representative Concentration Pathways, RCPs) corresponding to stabilization of radiative forcing after the 21st century at 4.5 W/m² (RCP4.5), rising radiative forcing crossing 8.5 W/m² at the end of 21st
85 century (RCP8.5), and peaking radiative forcing within the 21st century at 3.0 W/m² and declining afterwards (RCP2.6) (Moss et al., 2010).

Precipitation and air temperature are the fundamental environmental variables controlling climate and groundwater recharge processes, whose time series, simulated by the RCMs, are easily and largely applicable for the quantification of the groundwater recharge by empirical and numerical models. Ensembles of different GCMs/RCMs are recognized a suitable
90 approach for reducing the uncertainty of the results given by a single model (Sulis et al., 2012, Teutschbein & Seibert, 2012). For the same scope, temporal analyses are carried out at various time scales for a better assessment. Statistical downscaling techniques can increase further the spatial resolution of climate data up to the local scale, while a range of bias correction methods (Gudmundsson et al., 2012; Teutschbein & Seibert, 2012) have been developed to overcome the large biases in climate models, and can be used also for the quantification of the groundwater recharge through empirical models or water
95 budget approach.

3 Data and methods

3.1 Study area description

100 The territory of southern Italy is characterized by a high heterogeneity and complexity of geological-structural and hydrogeological features, due to the variety of sedimentary series forming the different tectonic units of the Apennine Chain and their tectonic relationships. The principal hydrogeological features of the southern Italy can be summarized in nine hydrogeological domains (De Vita et al., 2018) which, in decreasing order of relevance for what regards the mean annual specific groundwater yield (Figs. 1 and 2), can be identified as: a) Mesozoic carbonate series that, depending on

105 hydrogeological features, can be arranged in four subgroups: calcareous-siliceous, limestone, dolomitic, carbonate and Apulian foreland carbonate aquifers; b) Plio-Quaternary alluvial and epiclastic deposits; c) volcanic rocks and soils of Plio-Quaternary eruptive centres; d) Paleozoic crystalline-metamorphic rocks of the Calabrian arch; e) Cretaceous-Cenozoic basin series, which mainly constitute the minor mountainous or hilly reliefs of the southern Apennines.

In such interregional framework, the study area includes the entire portion of the western sector of the southern Apennines

110 (about 19,339 km^2), where Mesozoic carbonate series, forming high mountain ranges, outcrop and constitute very extended karst aquifers characterized by high permeability due to fracturing and karst phenomena (Figs. 1 and 2). These karst aquifers are characterized by limestone, limestone-dolomite and dolomite rocks, ranging in age from Triassic to Upper Cretaceous, belonging to the Apennine carbonate platform (Mostardini and Merlini, 1986) or the Campanian-Lucanian-Calabrian kinematic unit (Bonardi et al., 2009), derived from the tectonic disintegration of the carbonate platform that occurred during

115 the Miocene tectonic phases. In southern Italy, karst aquifers cover the 45% (Ruggeri et al., 2021) of the territory hosting the major groundwater resources which supply drinkable, industrial and thermo-mineral uses as well as contributing to the equilibrium of river ecosystems. This is favoured by the peculiar geological-structural, hydrogeological, geomorphological and climatological settings of the region which determine the occurrence of several high-permeability karst aquifers, with a high mean annual groundwater recharge and groundwater circulation rates.

120 Given their importance, many studies have been carried out on the karst aquifers of southern Italy regarding: i) hydrogeological characterization and the mapping of groundwater resources (Celico 1983; Petrella et al., 2015; De Vita et al., 2018); ii) groundwater recharge estimation at the different spatio-temporal scales and by terrestrial and satellite datasets (Allocca et al., 2014; 2015; Fusco et al., 2017; Ruggieri et al., 2021); iii) groundwater vulnerability to pollution (e.g. Tufano et al., 2022), microbial contamination and environmental impact of cattle grazing on karst groundwater (Allocca et al.,

125 2018). The continental carbonate units of the southern Apennines are characterized by groundwater resources of greater relevance, if compared to the carbonate units of the Apulian foredeep (eastern side of Fig. 1), because being tectonically juxtaposed and laterally confined by hydrostratigraphic units of lower permeability belonging to pre- and syn-orogenic Plio-Quaternary basin and flysch series. The Plio-Quaternary deposits, which include deposits of alluvial plains, coastal plains and intermontane basins are the most commonly outcropping (about 24,500 km^2). They are directly recharged by effective or

130 secondary infiltration from watercourses, thus receiving lateral groundwater inflow from the adjoining karst aquifer systems.

The lateral confinement of karst aquifers by low-permeability terrains constrains the groundwater circulation toward huge basal springs which are often characterized by high flows up to a few m³/s (Celico, 1983; Olarinoye et al., 2020; Cusano et al., 2022), and predisposed to the effective tapping. Therefore, karst aquifers represent the main source of groundwater for southern Italy, providing an estimated average annual water volume of approximately $4{,}100\times10^6$ m³ · year⁻¹ with a mean specific annual groundwater yield up to 0.035 m³ · s⁻¹ · km⁻² (De Vita et al., 2018; Fig. 2).

3.2 Climate models

To investigate the future climate projections and the related impacts on groundwater recharge processes over the study area (Fig. 3b), annual precipitation and mean air temperature data from the EURO-CORDEX simulations (Jacob et al., 2014) were achieved from the nodes of the Earth System Grid Federation (ESGF; https://esgf.llnl.gov/).

Specifically, 15 different combinations of RCMs and related GCMs driving data were selected (Table 2). RCMs selected belong to the realm EUR-11 with a resolution of 0.11° (about 12.5 km) (Fig. 3a). Accordingly, data available for the "historical experiment" period (from 1950/1970 to 2005) and scenarios (run from 2006 to 2099/2100) were analysed in this research. Moreover, for the future projections, two RCPs (Pachauri et al., 2014; Van Vuuren et al., 2011) were selected: RCP4.5 and RCP8.5, because they are widely used in studies regarding the assessment of climate change impacts, where the RCP8.5 is the most severe (business as usual), while the RCP4.5 is representative of intermediate conditions.

As a result, an ensemble of 15 RCM$_S$ (E15; Table 2) was reconstructed, re-projected in WGS84-UTM 33N and analysed.

3.3 Observed precipitation and air temperature time series (1950-1996)

In the southern Italy, as well as for the rest of the national territory, a hydrological monitoring has been carried out since 1921 by means of a dense monitoring network, managed by the SIMN governmental agency and consisting in a numerous series of rain gauges and air temperature stations. From 1921 to 1999, the activities carried out by the SIMN included the monitoring, survey, validation and dissemination of meteorological, hydrological and hydraulic data in annals and other types of publication.

In the study area, the management of the monitoring network was in charge of the Department of Naples of the SIMN, which operated in a territory covering a large part of southern Italy, comprising the study area (Fig. 3b). The meteorological monitoring network was provided initially by mechanical rain gauges, based on the accumulation of the daily rainfall, and air temperature stations which were managed by the people to which their maintenance was committed. Moreover, a systematic measurement of other hydrological observations, such as water levels of wells, lakes and rivers as well as river discharges, were carried out.

Starting from 1921, the number of rain gauges and air temperature stations was progressively increased and improved technologically until reaching a total of 423 stations in 1999. The recorded data, after a process of validation, were published in the annals by the aggregation of data from daily, to monthly and annual temporal scales. Moreover, the highest intensity rainfall events occurred in short time durations (less than 24 hours) were also reported in the annals.

The meteorological network undergone different changes during the period 1921-1999 due to the progressive increase of the number of stations as well as their discontinuous activity, because of temporary malfunctioning or abandonment during the World War II as well their relocation. These continuous changes of the monitoring network resulted in time series discontinuous in space and time.

Notwithstanding these issues, the huge database of historical meteorological data was considered very relevant for the comparison with RCMs data of the "historical experiments" periods (from 1950/1970 to 2005) and considered innovative for the regional scale of analysis, instead of the more common site-specific one. Therefore, annual precipitation and mean annual air temperature were extracted by the annals of the SIMN, made of public access by a dedicated project of Italian Institute for Environmental Protection and Research (ISPRA) (https://www.isprambiente.gov.it/it/progetti/cartella-progetti-in-corso/acque-interne-e-marino-costiere-1/progetti-conclusi/progetto-annali), and filed in a database covering the period 1950-1996. In detail, annual precipitation and mean annual air temperature data were extracted for each of the available monitoring stations, which were considered as observation points (OBS). The OBS data were used for a statistical comparison to the E15 ones at the regional scale, by considering both types of data comprised in each of the grid cells of the RCMs (~12 km) (Figs. 3a and 3b). A total of 143 RCMs grid cells were recognized comprising rain gauge stations, while 96 air temperature stations.

In order to represent the spatial and temporal variability of rain gauge and air temperature stations comprised in the cells of the RCMs, a representation in the form of heat map was carried out respectively (Figs. 4 and 5).

By the analysis of spatial and temporal distribution of rain gauges in the grid cells of RCMs (Fig. 3b) a minimum number of 100 functioning rain gauges in 1951 and 1991 and a maximum of 225 in 1978 is recognized (Fig. 4). The coverage of each grid cell of RCMs with at the least one rain gauge, up to six, prevails on cells with no rain gauges.

Regarding the spatial and temporal distribution of air temperature stations in the grid cells of RCMs (Fig. 5), the minimum number of 20 occurred in 1950 and a maximum of 96 in 1985. The coverage of each cell with no air temperature stations prevails on those comprising at least one. The latter were recognized encompassing up to four air temperature stations for each grid cell. The lower spatial density of air temperature stations in comparison to that of rain gauges is due to the lower spatial variability of the air temperature which is mostly controlled by the altitude only.

3.4 RCMs processing: validation, bias assessment and correction

All the RCM$_S$ precipitation and air temperature data were pre-processed with the Climate Data Operators (CDO) software (Schulzweida, 2022), which is a collection of operators and tools for standard processing of climate and forecast model data in NetCDF format. The operators include arithmetic functions, data selection and subsampling tools and spatial interpolation. For each model, the pre-processing has involved the aggregation of the NetCDF datasets and the conversion of the units of precipitation (from $kg \cdot m^2 \cdot s^{-1}$ to $mm \cdot h^{-1}$) and temperature (from K to °C). Therefore, a subset of data related to the area of the southern Apennines was extracted (Fig. 3b).

195 RCMs data needs correction of systematic errors (*bias correction*), which is performed considering a period (validation period) where observed (OBS) and modelled time series are available and overlapped (D'Oria et al., 2018).

Different methodologies for the bias correction of climatic variables were developed (Teutschbein & Seibert, 2012), depending on the choice of the method on both the type of the observed data available and the goal of the study (D'Oria et al., 2018).

200 Bias-correction methods require continuous daily or monthly time-series over a period of at least 30 years (Trzaska & Schnarr, 2014). The purpose of this stage of data processing was to assess the differences existing between the RCM_S "historical experiments" periods datasets and the measured data (OBS) in the selected validation period (1950-1996). This assessment was assumed leading to the recognition of an empirical criterion applicable as a calibration of RCMs data, to be used for the estimation of future scenarios of hydrological variables controlling groundwater recharge of karst aquifers of 205 southern Italy. The elaboration was performed with the High-level functions NetCDF Library Package of MATLAB® (R2021b) applicable for reading and processing climate variables from netCDF data files.

In the present work, a method based on inferential statistical studies of the bias was adopted. In this view, in order to allow the comparison between the E15 and OBS data, two pairs of datasets were created for each year of the validation period (1950-1996), which were based on the recognition of grid cells of the RCM model within which OBS precipitation (OBS_P)
210 and OBS air temperature (OBS_T) resulted available (Figs. 4, 5, 6a and 6b). Specifically, the E15 and OBS datasets adopted for this study consider the total annual precipitation and the mean air temperature values.

For a specific year, OBS_P and OBS_T given for each cell grid were compared with the E15 precipitation ($E15_P$) and air temperature ($E15_T$) data known for the same grid cell (Figs. 5a and 5b). In the case of multiple stations occurring in the same grid cell, mean values of OBS_P and OBS_T were calculated and compared with the corresponding $E15_P$ and $E15_T$ data. After
215 the reconstruction of the datasets, the *bias* analysis between $E15_P$ and OBS_P and between $E15_T$ and OBS_T was carried for every grid cell at the annual scale by the equation Eq. (1):

$$Bias_{P,T,t}(j) = \frac{(Model_{P,T,t}(j) - OBS_{P,T,t}(j))}{OBS_{P,T,t}(j)}, \qquad (1)$$

where $Model_{P,T,t}(j)$ is the value of $E15_P$ or $E15_T$ and $OBS_{P,T,t}(j)$ is the observed value of precipitation or temperature for
220 the year t (t= 1950, 1951...1996) in the jth grid cell.

Then, the mean value of the bias over the generic t_{-year} ($\overline{Bias_{P,T,t}}$) and the whole area, was calculated as Eq (2):

$$\overline{Bias_{P,T,t}} = \frac{\sum_{j=1}^{n} Bias_{P,T}(j)}{\sum_{j=1}^{n} j}, \qquad (2)$$

In which n indicates the number of grid cells considered. Finally, the bias-corrected annual value of the E15 ($Model^*_{P,T,t}(j)$) is then evaluated as Eq (3):

225 $$Model^*_{P,T,t}(j) = Model_{P,T,t}(j) * (1 - \overline{Bias_{P,T}}), \qquad (3)$$

This method was applied to correct the E15$_P$ and E15$_T$ data over the validation period (1950-1996) and the future period under both the RCP4.5 and RCP8.5 pathway scenarios.

3.5 Hydro-climatological scenarios

230   The evaluation of the long-term effects of climate change on hydrological variables controlling groundwater recharge of karst aquifers was carried out considering the E15 bias-corrected values of precipitation and air temperature. Among the different hydrogeological domains, the spatial analyses were carried out on the areas of karst aquifers (Figs. 3a and 3b), which were considered the most relevant for the assessment of the impact of climate change on groundwater recharge due to their hydrogeological relevance. Accordingly, all the E15 grid cells intersecting the boundaries of the karst aquifers were extracted from the whole E15 dataset, and time series of mean annual precipitation and air temperature were created for

235   reconstructing a complete time series including both the "historical experiment" period (1950-2005) and scenarios (2006-2100) under both the RCP4.5 and RCP8.5 pathways.

The evaluation of the climate change impact on groundwater recharge was assessed through the application of the hydrological budget equation Eq (4):

$$P_{tj} = ETR_{tj} + Ie_{tj} + R_{tj} , \qquad (4)$$

240   where, P_{tj} is the precipitation, ETR_{tj} is the actual evapotranspiration, Ie_{tj} is the effective infiltration or groundwater recharge and R_{tj} is the runoff, respectively related to the t-*year* and j-*cell*.

Given its formulation and validation for Mediterranean hydrographic basins, the ETR was estimated by the Turc empirical formula (Turc, 1955) Eq (5):

$$ETR_{t,j} = \frac{P_{t,j}}{\sqrt{0.9 + \left(\frac{P_{t,j}}{300 + 25*T_{t,j} + 0.05*T_{t,j}^3}\right)^2}} , \qquad (5)$$

245   where $P_{t,j}$ is the total annual precipitation (mm) and $T_{t,j}$ is the mean annual air temperature (°C), both for the j-*cell*.

From Eqs. 4 and 5, the effective precipitation $Pe_{t,j}$ of the t-*year* and j-*cell* was considered as a proxy hydrological parameter describing the amount of precipitation potentially available groundwater recharge process and, therefore, useful for assessing the related effects of climate change scenarios Eq. (6):

$$Pe_{tj} = P_{tj} - ETR_{tj} = +Ie_{tj} + R_{tj} , \qquad (6)$$

250   The reconstruction of Pe time series until 2100 is considered a fundamental step to assess the groundwater recharge by the application of empirical (Allocca et al., 2014) or numerical models (D'Oria et al., 2019).

Finally, to investigate the variation of Pe relatively to the "historical experiment" period (1950-2005), the Mean Annual Effective Precipitation Index (MAEPI) (De Vita et al., 2012) was calculated for each year of the time series and the whole area, as follows Eq. (7):

255    $$MAEPI_t = \frac{Pe_t - Pe\,Hist_t}{Pe\,Hist_t} , \qquad (7)$$

where MAEPI$_t$ is the Mean Annual Effective Precipitation Index for the t-$_{year}$ (%), Pe$_t$ is the Effective Precipitation for the t-$_{year}$ and Pe Hist$_i$ is the Mean Annual Effective Precipitation of the whole E15 time series, corresponding to the "historical experiment" period (1950-2005), and the whole area.

4. Results

4.1 RCMs bias assessment

The bias assessment in the validation period (1950-1996), based on an inferential statistic approach, led to the quantification of accuracy of RCMs in terms of overestimation or underestimation between precipitation and air temperature values of the single RCMs considered (Table 2) and corresponding OBS (Eq. 1; Table 3; Figs. 7 and 8) as well as between E15$_P$ and E15$_T$ and the OBS$_P$ and OBS$_T$, respectively (Table 4; Fig. 9).

In detail, a total of 143 RCM$_S$ grid cells were extracted for precipitation (Fig. 6a) and 96 for air temperature (Fig. 6b), considering in both cases only grid cells comprising monitoring stations in the whole validation period (1950-1996), even with a discontinuous functioning. Although precipitation and air temperature values of single RCM sometimes differ significantly from the corresponding OBS, the matching was found in general more accurate considering E15 values (Fig. 9). In detail, the comparison of single RCMs with OBS reveals that HIRHAM5 and RCA4 showed the highest difference, while CCLM4-8-17 and RACMO22E the greatest similarities (Fig. 7); instead, the E15 (Table 2) showed a relevant matching when compared to OBS.

Both E15$_P$ and OBS$_P$ were found statistically distributed with a log-normal model (Fig. 9a), showing an overestimation of E15$_P$ by an average of 7% (0.070; Table 4). Conversely, air temperatures values of single RCMs were recognized in average lower than the corresponding OBS values (Fig. 8), showing also a quite different statistical distribution for all RCM$_S$ (Table 3). Even E15$_T$ values are on average 2 °C lower than OBS$_T$. This aspect appears as dependent on the intrinsic errors of the RCMs. These differences in air temperature between RCMs and OBS were also observed in preceding studies carried out over the same region (Bucchignani et al., 2016; Zollo et al., 2016). Specifically, by comparing E15$_T$ and OBS$_T$ it was observed that in both cases the values assume a normal distribution (Fig. 9a) and that E15$_T$ underestimates the actual data by 16% (-0.160; Table 5).

4.2 RCM bias-correction

To investigate the future effects of climate change on groundwater recharge of the principal aquifer systems of southern Italy, we considered the ensemble mean of 15 RCM$_S$ (Table 2).

The E15$_P$ and E15$_T$ were bias-corrected according to the Eq. 2 and using the results obtained with the bias inferential statistical analysis (Tabs. 4 and 5). For both E15$_P$ and E15$_T$, the evaluation of the bias-correction was performed by applying the Eq. 1 on the bias-corrected E15 data (Fig. 9b).

After the correction between the OBS$_P$ and the E15$_P$, the bias decreased leading to an overestimation of E15$_P$ of about 0.4% (0.004) in average (Figs. 9b and 9c). Instead, the corrected E15$_T$ values showed an underestimation of 2.4% (Table 5) (Figs. 9b and 9c).

4.3 Hydro-climatological scenarios (2006-2100)

290 The annual corrected values of E15$_P$ and E15$_T$ were used to reconstruct a continuous time series of the "historical experiment" period from 1950 to 2005 and of the scenarios from 2006 to 2100, for both RCP4.5 and RCP8.5 pathways, over the entire domain of the karst aquifers of southern Italy (Fig. 10).

Precipitation scenarios show a decreasing trend for both pathways, with strong interannual variations and rates of the RCP8.5 lower than those of the RCP4.5 one (Fig. 11a).

295 Both scenarios project an increase in air temperature, in particular the pathway RCP8.5 shows the largest increase of the mean value up to about 4 °C at the end of the century (Fig. 11b). Instead, the scenario related to the pathway RCP4.5 projects an increase up to 2 °C of the mean value. These differences are clearly recognizable from 2040, where a clear divergence in the trends of the time series occurs.

For E15$_P$ and E15$_T$ time series under both pathway scenarios, a confidence interval (error) was reconstructed considering the

300 value of the standard deviation of the bias estimated respectively in comparison to OBS$_P$ and OBS$_T$, thus corresponding to a probability interval of 68.27%.

The E15$_P$ and E15$_T$ time series of both pathways were applied for quantifying the scenarios of ETR and Pe. According to the general increase in air temperature, scenarios of ETR (2006-2110) reveals a progressive rise for both RCP pathways (Fig. 12a).

305 As a first result, Pe time series show a marked decreasing trend for both RCP8.5 and RCP4.5 pathways, with the most severe condition for the RCP8.5 one (Fig. 12b). This is clearly confirmed by the comparison of the cumulative frequency distribution (%) of Pe time series in the "historical experiment" period (1950-2005) and Pe time series of scenarios from 2045 to 2100 of both pathways (Fig. 13a); in detail, it is possible to assess that the median values (frequency of 50%) amount to 510 mm for the "historical experiment" period (1950-2005), and to 415 mm and 320 mm for RCP4.5 and RCP8.5

310 pathways (2006-2100), respectively.

The trend of MAEPI shows a quite stable decadal trend in the "historical experiment" period (1950 – 2005), whose global average is about 538.8 mm (Fig. 13b), while relevant decreasing trends for the long-trend projections (2006-2100) of both pathways scenarios indicating a decrease of the 11-yrs moving average down to -20% for RPC 4.5 and -50% for RPC 8.5. In detail, the projected time series of both pathways show (starting from 2040) for the RPC 4.5 a stabilisation of the MAEPI 11-

315 yrs moving average around a value 20% lower than the average of the "historical experiment" period (538.8 mm), and an enhancement of the decreasing trend for the RPC 8.5.

Moreover, remarkable annual and complexly cyclical fluctuations around the 11-yrs moving average of Pe were observed within the "historical experiment" period (1950-2005) and scenarios (2006-2100) periods time series (Fig. 13b). In

comparison to the Pe mean value of the whole "historical experiment" period (538.8 mm), MAEPI ranges in the "historical
320   experiment" period from a minimum -23.4% (1965) to a maximum +30.47% (1980). Moreover, MAEPI showed two
pluriannual phases with values above the mean value of the whole "historical experiment" period (1950-2005),
corresponding respectively to periods 1955-1959 and 1971-1981, and two phases below this mean value, corresponding to
the periods 1960-1970 and 1982-2000.

Similarly, MAEPI estimated for the future scenario periods (2005-2110) for both pathways RCP4.5 and RCP8.5 showed
325   marked inter-annual fluctuations overlapping on the decreasing trends, with a fluctuation range of about ± 15% around the
11-yrs moving average, which appear reaching and exceeding the mean value of the "historical experiment" period (538.8
mm) only in few years until 2070, for the RPC 4.5 pathway scenario, and until 2040, for the PRC 8.5 one.

5 Discussion

In this work, an application of RCM climate models is proposed as a practical tool to assess, analyse and predict the effects
330   of climate change until the end of the current century on the hydrological variables that control groundwater recharge
processes in the principal aquifer systems of southern Italy, which are chiefly represented by karst aquifers.

Among the most relevant outcomes of this research, the ensemble of RCMs (E15) for precipitation ($E15_P$) and air
temperature ($E15_T$) overperforms the representation of observed precipitation (OBS_P) and air temperature (OBS_T) data, with
respect to the individual models. Data were recorded over the whole region in the validation period (1950-1996) by the
335   SIMN national meteorological network, even discontinuously in space and time. According to the regional scale of analysis,
needed for the hydrogeological purposes, the research was focused on the comparison of $E15_P$ and $E15_T$ to OBS_P and OBS_T
in order to assess statistical differences, namely the bias between the modelled and observed data. In such a view, this work
can be conceived novel in the field of application of RCMs because compares modelled and observed meteorological data on
a regional scale by accounting for the spatial and temporal discontinuity of observed time series, which is a common issue of
340   the regional meteorological networks.

The *bias-correction* method proposed in this study is based on inferential statistical analysis of precipitation and air
temperature values of both E15 and OBS data, which are discontinuous in space and time. The method proposed allow the
management of OBS data aggregated at the annual scale for the estimation of the groundwater recharge, thus not requiring
precipitation data aggregated at the daily or monthly time scales with continuous time series as needed for other bias-
345   correction methods such as Linear Scaling (LS) (Wetterhall et al., 2012; Schmidli et al., 2006), Local Intensity Scaling
(LOCI) (Schmidli et al., 2006; Themeßl et al., 2010), and the Quantile Mapping (QM) (Wetterhall et al., 2012).

Precipitation and air temperature rates resulting from the E15, related to scenarios of both RCP8.5 and RCP4.5 pathways,
show trends consistent with those described in various climatological studies carried out in the central and southern Italy
(Braca et al., 2019; Bucchignani et al., 2016; Zollo et al., 2016). In the same way, MAEPI derived by E15 variables, show a
350   complex periodicity with decadal and overlapped interannual fluctuations. Considering the validation period (1950-1996),

these complex fluctuations of both precipitation (P) and effective precipitation (Pe) were already recognized to be related to the North Atlantic Oscillation (De Vita et al., 2012).

Similarly, from the predictive scenarios, it can be seen how ETR and Pe are strongly controlled by the long-term decrease in precipitation and increase in air temperature rates, especially considering the scenario regulated by the RCP8.5 pathways. In
355 addition, the integrated analysis of MAEPI showed, by the filtering with the 11-yrs moving average, a complex periodicity of the time series with decreasing cycles until the end of the century for both RCP scenarios with a total decrease of the moving average value down to -20% for RCP4.5 and to -50% for RCP8.5.

6 Conclusions

The definition of climate change scenarios in terms of air temperature (T), precipitation (P), actual evapotranspiration (ETR)
360 and effective precipitation Pe (P – ETR) on principal aquifer systems of southern Italy, under different RCP scenarios, was the main focus of this study.

A methodology is presented, aimed to compare and correct the atmospheric variables provided by an ensemble mean of 15 RCMs (E15) at 0.11° (~12 km) grid spatial resolution, with observational values provided by a dense meteorological network, which functioned discontinuously in space and time over the period 1950-1996.
365 The E15 in terms of precipitation and air temperature shows a frequency distributions similar to those of observed data (OBS), resulting statistically valid.

E15 projections show a reduction in precipitation and an increase in air temperature under both RCPs, with a divergence point between the two scenarios occurring by about 2040.

As a result, Pe, which is considered as a proxy of groundwater recharge, is characterized by significant inter-annual
370 fluctuations and shows decreasing trends under both RCP scenarios, reaching a decrease of the 11-yrs moving average down to -20%, for RCP4.5, and -50% for the "business as usual" RCP8.5.

In summary, the proposed methodology can be considered valid for analysing the effects of climate variations at the regional scale on the selected hydrological variables (P, T, ETR and Pe) that control groundwater recharge processes of principal aquifer systems of the southern Italy, from which the socio-economic development and environmental conservation of
375 groundwater dependant ecosystems are reliant on. This research has revealed the potential of RCMs in the definition of groundwater recharge scenarios under future changing climate conditions, highlighting the relevant vulnerability of principal aquifer systems of southern Italy, among which the karst ones are the most important.

Data availability

All raw data can be provided by the corresponding authors upon request.
380

Author contributions.

Conceptualization: DL, PDV, VA and EB; data curation: DL, PDV, EB, MM, DC and VA; methodology: DL, PDV, MM, EB, VA and DC; software: DL, MM and DC; supervision: PDV, EB, MM, VA, visualization: DL, DC; writing—original draft: DL, PDV, EB, VA and DC; writing—review & editing: DL, PDV, EB, VA and DC.

385 All authors read and approved the final manuscript.

Competing interests.

The authors declare that they have no conflict of interest.

390 **Acknowledgements**

Authors acknowledge the funding of the research by the PhD Program of Dipartimento di Scienze della Terra, dell'Ambiente e delle Risorse (DiSTAR), Università di Napoli Federico II (36th cycle).

References

Allocca, V., De Vita, P., Manna, F., and Nimmo, J. R..: Groundwater recharge assessment at local and episodic scale in a
395 soil mantled perched karst aquifer in southern Italy, Journal of Hydrology, 529, 843-853, 2015.

Allocca, V., Manna, F., and De Vita, P..: Estimating annual groundwater recharge coefficient for karst aquifers of the southern Apennines (Italy), Hydrology and Earth System Sciences, 18, 803-817, 2014.

Allocca V., Marzano E., Tramontano M., Celico F..: Environmental impact of cattle grazing on a karst aquifer in the southern Apennines (Italy): quantification through the grey water footprint, Ecological Indicators, 93, 830-837, 2018.

400 Bonardi, G., Ciarcia, S., Di Nocera, S., Matano, F., Sgrosso, I., and Torre, M..: Carta delle principali unità cinematiche dell'Appennino meridionale, Nota illustrativa. Bollettino della Società Geologica Italiana, 128, 47-60, 2009.

Braca, G., Bussettini, M., Ducci, D., Lastoria, B., and Mariani, S..: Evaluation of national and regional groundwater resources under climate change scenarios using a GIS-based water budget procedure. Rendiconti Lincei. Scienze Fisiche e Naturali, 30, 109-123, 2019.

405 Bucchignani, E., Montesarchio, M., Zollo, A. L., and Mercogliano, P..: High-resolution climate simulations with COSMO-CLM over Italy: Performance evaluation and climate projections for the 21st century, International Journal of Climatology, 36(2), 735–756, 2016.

Celico, P. B..: Idrogeologia dei massicci carbonatici, delle piane quaternarie e delle aree vulcaniche dell'Italia centro-meridionale: Marche e Lazio meridionali, Abruzzo, Molise e Campania, Cassa per il Mezzogiorno, 1983.

410 Cusano D., Allocca V., Coda S., Lepore D., Vassallo M., De Vita P..: The survey of Italian springs by the National Hydrographic Service, a forgotten database. Structuring and analysis of a dataset of Campania springs (southern Italy), Italian Journal of Groundwater, 11(2), 31-41 https://doi.org/10.7343/as-2022-571, 2022.

De Vita, P., Allocca, V., Celico, F., Fabbrocino, S., Cesaria, M., Giuseppina, M., Ilaria, M., Vincenzo, P., Scalise, A. R., Summa, G., Tranfaglia, G., and Pietro, C..: Hydrogeology of continental southern Italy, Journal of Maps, 14(2), 230–241,
415 https://doi.org/10.1080/17445647.2018.1454352, 2018.

De Vita, P., Allocca, V., Manna, F., and Fabbrocino, S..: Coupled decadal variability of the North Atlantic Oscillation, regional rainfall and karst spring discharges in the Campania region (southern Italy), Hydrology and Earth System Sciences, 16(5), 1389-1399, 2012

D'Oria, M., Ferraresi, M., and Tanda, M. G..: Quantifying the impacts of climate change on water resources in northern
420 Tuscany, Italy, using high-resolution regional projections, Hydrological Processes, 33(6), 978–993, https://doi.org/10.1002/hyp.13378, 2019.

D'Oria, M., Tanda, M. G., Todaro, V..: Assessment of local climate change: Historical trends and RCM multi-model projections over the Salento Area (Italy), Water (Switzerland), 10(8), https://doi.org/10.3390/w10080978, 2018.

Fernández, J., Frías, M. D., Cabos, W. D., Cofiño, A. S., Domínguez, M., Fita, L., Gaertner, M. A., García-Díez, M.,
425 Gutiérrez, J. M., Jiménez-Guerrero, P., Liguori, G., Montávez, J. P., Romera, R., and Sánchez, E..: Consistency of climate change projections from multiple global and regional model intercomparison projects, Climate Dynamics, 52(1–2), 1139–1156, https://doi.org/10.1007/s00382-018-4181-8, 2019.

Fusco F., Allocca V., De Vita F..: Hydro-geomorphological modelling of ash-fall pyroclastic soils for debris flow initiation and groundwater recharge in Campania (southern Italy), Catena 158, 235–249, 2017.

430 Giorgi, F., Jones, C., and Asrar, G. R..: Addressing climate information needs at the regional level: the CORDEX framework. World Meteorological Organization (WMO) Bulletin, 58(3), 175, 2009.

Green, T. R., Taniguchi, M., Kooi, H., Gurdak, J. J., Allen, D. M., Hiscock, K. M., ... and Aureli, A..: Beneath the surface of global change: Impacts of climate change on groundwater, Journal of Hydrology, 405(3-4), 532-560, 2011.

Gudmundsson, L., Bremnes, J. B., Haugen, J. E., and Engen-Skaugen, T..: Hydrology and Earth System Sciences Technical
435 Note: Downscaling RCM precipitation to the station scale using statistical transformations-a comparison of methods, Hydrol. Earth Syst, Sci, 16, 3383–3390, https://doi.org/10.5194/hess-16-3383-2012, 2012.

Holman, I. P., Allen, D. M., Cuthbert, M. O., and Goderniaux, P..: Towards best practice for assessing the impacts of climate change on groundwater, Hydrogeology Journal, 20(1), 1–4, https://doi.org/10.1007/s10040-011-0805-3, 2012.

Jacob, D., Petersen, J., Eggert, B., Alias, A., Christensen, O. B., Bouwer, L. M., Braun, A., Colette, A., Déqué, M.,
440 Georgievski, G., Georgopoulou, E., Gobiet, A., Menut, L., Nikulin, G., Haensler, A., Hempelmann, N., Jones, C., Keuler, K.,

Kovats, S., … Yiou, P..: EURO-CORDEX: New high-resolution climate change projections for European impact research, Regional Environmental Change, 14(2), 563–578, https://doi.org/10.1007/s10113-013-0499-2, 2014.

Mostardini, F., and Merlini, S..: Appennino centro meridionale, sezioni geologiche e proposta di modello strutturale. [Central-southern Apennine, geological crosssections and proposal of a structural model], Memorie Società Geologica
445 Italiana, 35, 177–202, 1986.

Kurylyk, B. L., and MacQuarrie, K. T. B..: The uncertainty associated with estimating future groundwater recharge: A summary of recent research and an example from a small unconfined aquifer in a northern humid-continental climate, Journal of Hydrology, 492, 244–253, https://doi.org/10.1016/j.jhydrol.2013.03.043, 2013.

450 Nerantzaki, S. D., and Nikolaidis, N. P..: The response of three Mediterranean karst springs to drought and the impact of climate change, Journal of Hydrology, 591, 125296, 2020.

Olarinoye T., Gleeson T., Marx V., Seeger S., Adinehvand R., Allocca V., Andreo B., James Apaéstegui J. Apolit C., Arfib B., Auler A., Barberá J.A., Batiot-Guilhe C., Bechtel T., Binet S., Bittner D., Blatnik M., Bolger T., Brunet P., Charlier J.-B, Chen Z., Chiogna G., Coxon G., De Vita P., Doummar J., Epting J., Fournier M., Goldscheider N., Gunn J., Guo F., Guyot
455 J.L., Howden N., Huggenberger P., Hunt B., Jeannin P.Y., Jiang G., Jones G., Jourde H., Karmann I., Koit O., Kordilla J., Labat D., Ladouche B., Liso I.L., Liu Z., Massei N., Mazzilli N., Mudarra M., Parise M., Pu J., Ravbar N., Sanchez L.H., Santo A., Sauter M., Sivelle V., Skoglund R.Ø., Stevanovic Z., Wood C., Worthington S., and Hartmann A..: Global karst springs hydrograph dataset for research and management of the world's fastestflowing groundwater, Scientific Data 7:59, https://doi.org/10.1038/s41597-019-0346-5, 2020.

460 Pachauri, R. K., Allen, M. R., Barros, V. R., Broome, J., Cramer, W., Christ, R., Church, J. A., Clarke, L., Dahe, Q., and Dasgupta, P..: Climate change 2014: Synthesis report, Contribution of Working Groups I, II and III to the fifth assessment report of the Intergovernmental Panel on Climate Change, Ipcc, 2014.

Pardo-Igúzquiza, E., Collados-Lara, A. J., and Pulido-Velazquez, D..: Potential future impact of climate change on recharge in the Sierra de las Nieves (southern Spain) high-relief karst aquifer using regional climate models and statistical corrections,
465 Environmental Earth Sciences, 78(20), 1-12, 2019.

Petrella, E., Aquino, D., Fiorillo, F., Celico, F..: The effect of low-permeability fault zones on groundwater flow in a compartmentalized system. Experimental evidence from a carbonate aquifer (Southern Italy), Hydrol. Process., 29, 1577-1587, doi:10.1002/hyp.10294, 2015.

Pulido-Velazquez, D., García-Aróstegui, J. L., Molina, J. L., and Pulido-Velazquez, M..: Assessment of future groundwater
470 recharge in semi-arid regions under climate change scenarios (Serral-Salinas aquifer, SE Spain), Could increased rainfall variability increase the recharge rate?, Hydrological processes, 29(6), 828-844, 2015.

Pulido-Velazquez, D., Collados-Lara, A. J., and Alcalá, F. J..: Assessing impacts of future potential climate change scenarios on aquifer recharge in continental Spain, Journal of Hydrology, 567, 803-819, 2018.

Ruggieri, G., Allocca, V., Borfecchia, F., Cusano, D., Marsiglia, P., and De Vita, P..: Testing evapotranspiration estimates
475 based on MODIS satellite data in the assessment of the groundwater recharge of karst aquifers in southern Italy, Water,
13(2), 118, 2021.

Schmidli, J., Frei, C., and Vidale, P. L..: Downscaling from GCM precipitation: a benchmark for dynamical and statistical
downscaling methods, International Journal of Climatology: A Journal of the Royal Meteorological Society, 26(5), 679-689,
2006.
480

Schulzweida, U..: CDO User Guide, https://doi.org/10.5281/zenodo.7112925, 2022.

Stevanović, Z..: Karst aquifers in the Arid World of Africa and the Middle East: sustainability or humanity?, Karst Water
Environment: Advances in Research, Management and Policy, 1-43, 2018.

Stigter, T. Y., Ribeiro, L., Samper, J., Fakir, Y., Pisan, B., Tomé, S., and Fonseca, L..: Comparative assessment of climate
485 change impacts on coastal groundwater resources and dependent ecosystems in the Mediterranean, Reg Environ change
(submitted), 2012.

Stigter, T. Y., Nunes, J. P., Pisani, B., Fakir, Y., Hugman, R., Li, Y., and El Himer, H..: Comparative assessment of climate
change and its impacts on three coastal aquifers in the Mediterranean, Regional environmental change, 14(1), 41-56, 2014.

Sulis, M., Paniconi, C., Marrocu, M., Huard, D., and Chaumont, D..: Hydrologic response to multimodel climate output
490 using a physically based model of groundwater/surface water interactions, Water Resources Research, 48(12), 2012.

Taylor, R. G., Scanlon, B., Döll, P., Rodell, M., Van Beek, R., Wada, Y., and Treidel, H..: Ground water and climate change,
Nature climate change, 3(4), 322-329, 2013.

Teutschbein, C., and Seibert, J..: Bias correction of regional climate model simulations for hydrological climate-change
impact studies: Review and evaluation of different methods, Journal of Hydrology, 456–457, 12–29.
495 https://doi.org/10.1016/J.JHYDROL.2012.05.052, 2012.

Themeßl, M., & Gobiet, A..: Empirical-statistical downscaling and model error correction of daily temperature and
precipitation from regional climate simulations and the effects on climate change signals, Proceedings of the EGU General
Assembly, Vienna, Austria, 2-7, 2010.

Trzaska, S., and Schnarr, E..: A review of downscaling methods for climate change projections, United States Agency for
500 International Development by Tetra Tech ARD, September, 1–42, 2014.

Tufano R., Allocca V., Coda S., Cusano D., Fusco F., Nicodemo F., Pizzolante A., De Vita P..: Groundwater vulnerability of
principal aquifers of the Campania region (southern Italy), Journal of Maps, 16:2, 565-576, 2020.

Turc, L..: Le bilan d'eau des sols: Relations entre les précipitations, l'évaporation et l'écoulement. Journées de l'hydraulique,
3(1), 36–44, 1955.

505 Van Vuuren, D. P., Edmonds, J., Kainuma, M., Riahi, K., Thomson, A., Hibbard, K., Hurtt, G. C., Kram, T., Krey, V., and
Lamarque, J.-F..: The representative concentration pathways: An overview, Climatic change, 109, 5–31, 2011.

Voulanas, D., Theodossiou, N., & Hatzigiannakis, E..: Assessment of potential hydrological climate change impacts in the Kastoria basin (Western Macedonia, Greece) using EURO-CORDEX regional climate models, GLOBAL NEST JOURNAL, 23(1), 43, 2021.

510 Wetterhall, F., Pappenberger, F., He, Y., Freer, J., and Cloke, H. L..: Conditioning model output statistics of regional climate model precipitation on circulation patterns, Nonlinear Processes in Geophysics, 19(6), 623-633, 2012.

Zollo, A. L., Rillo, V., Bucchignani, E., Montesarchio, M., and Mercogliano, P..: Extreme temperature and precipitation events over Italy: assessment of high-resolution simulations with COSMO-CLM and future scenarios, International Journal of Climatology, 36(2), 987-1004, 2016.

515

520
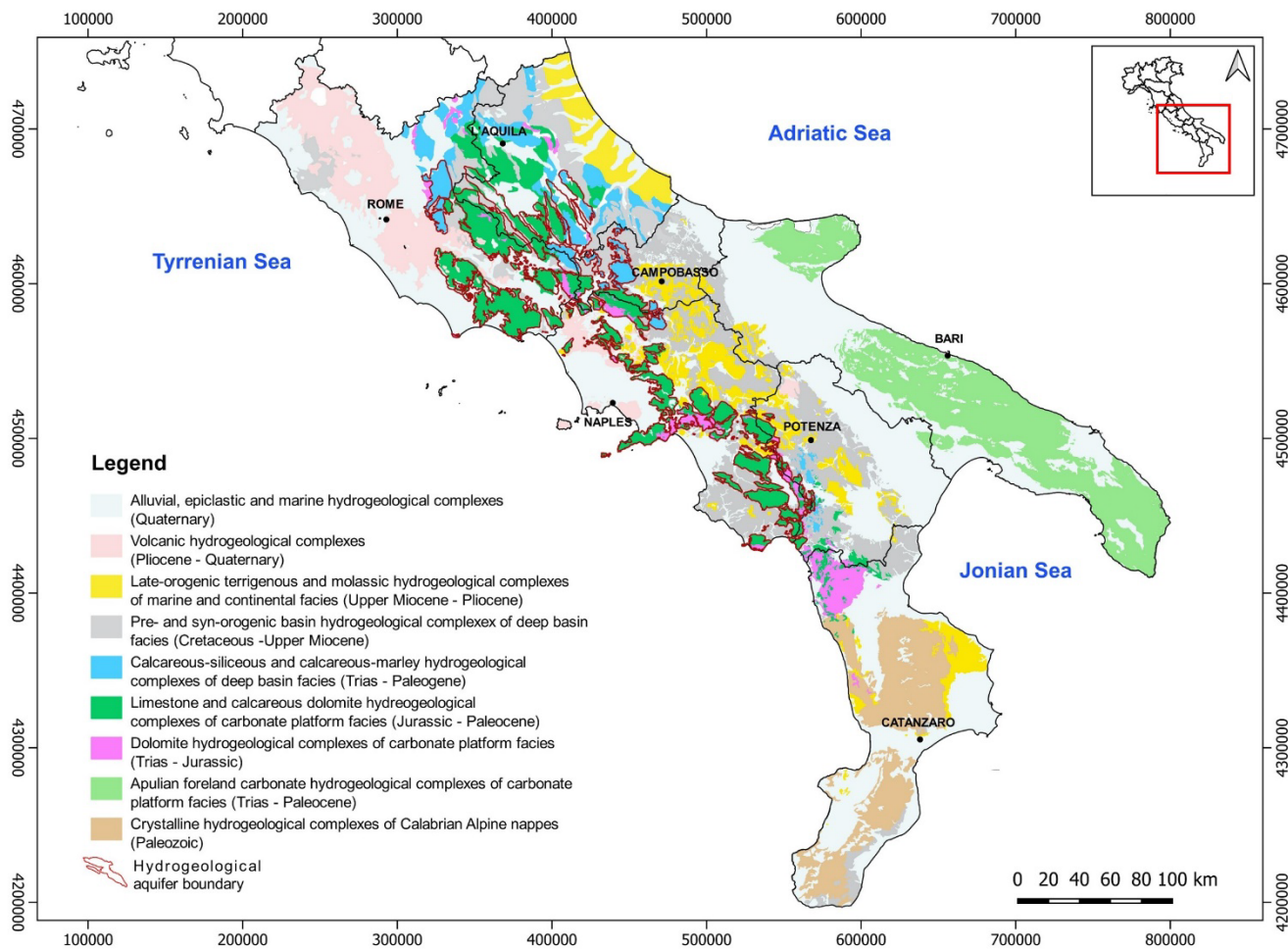
Figure. 1: Hydrogeological map of the continental southern Italy (redrawn from De Vita et al., 2018) showing the nine principal hydrogeological domains. Hydrogeological boundaries of karst aquifers are also shown.

525

530
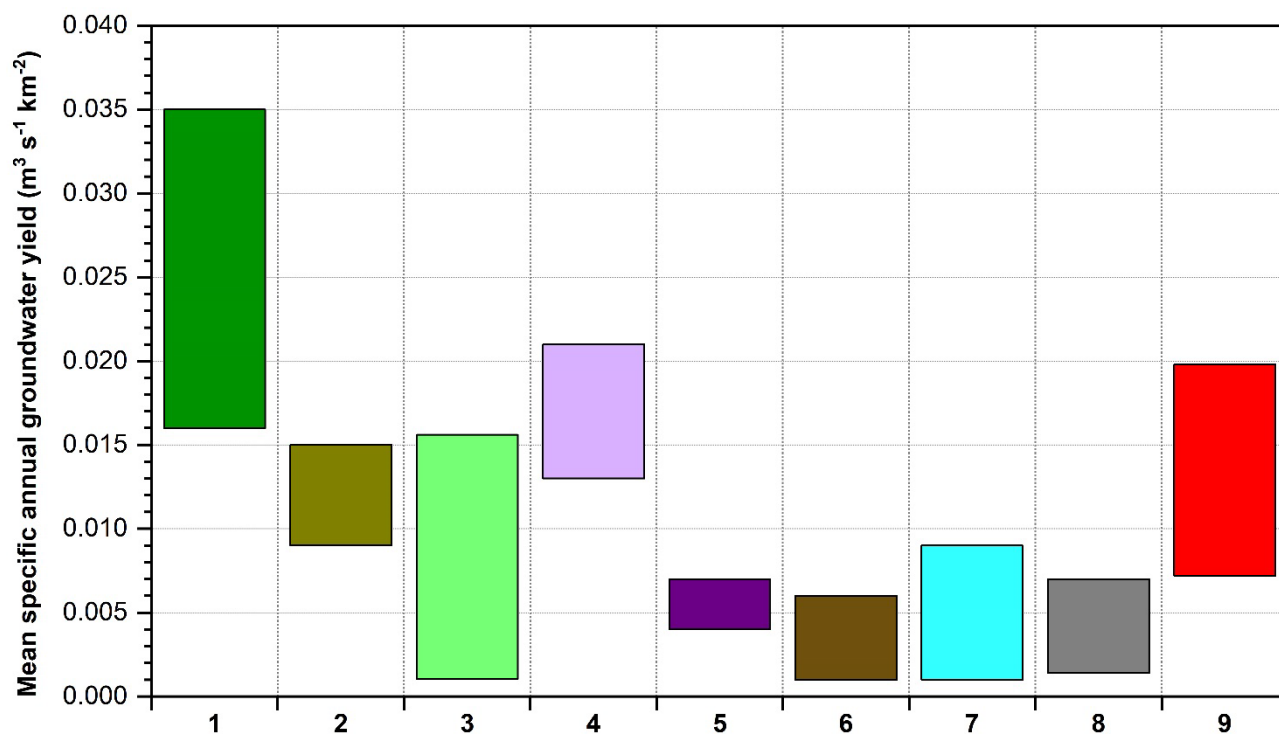
Figure 2: Mean specific annual groundwater yield of hydrogeological domains estimated for the southern Italy (redrawn from De Vita et al., 2018). Keys to legend: 1) Limestone and calcareous dolomite units; 2) Calcareous-marly units; 3) Apulian carbonate units; 4) Dolomite units; 5) Crystalline units; 6) Terrigenous units; 7) Alluvial units; 8) Pre and syn-orogenic units; 9) Volcanic units.
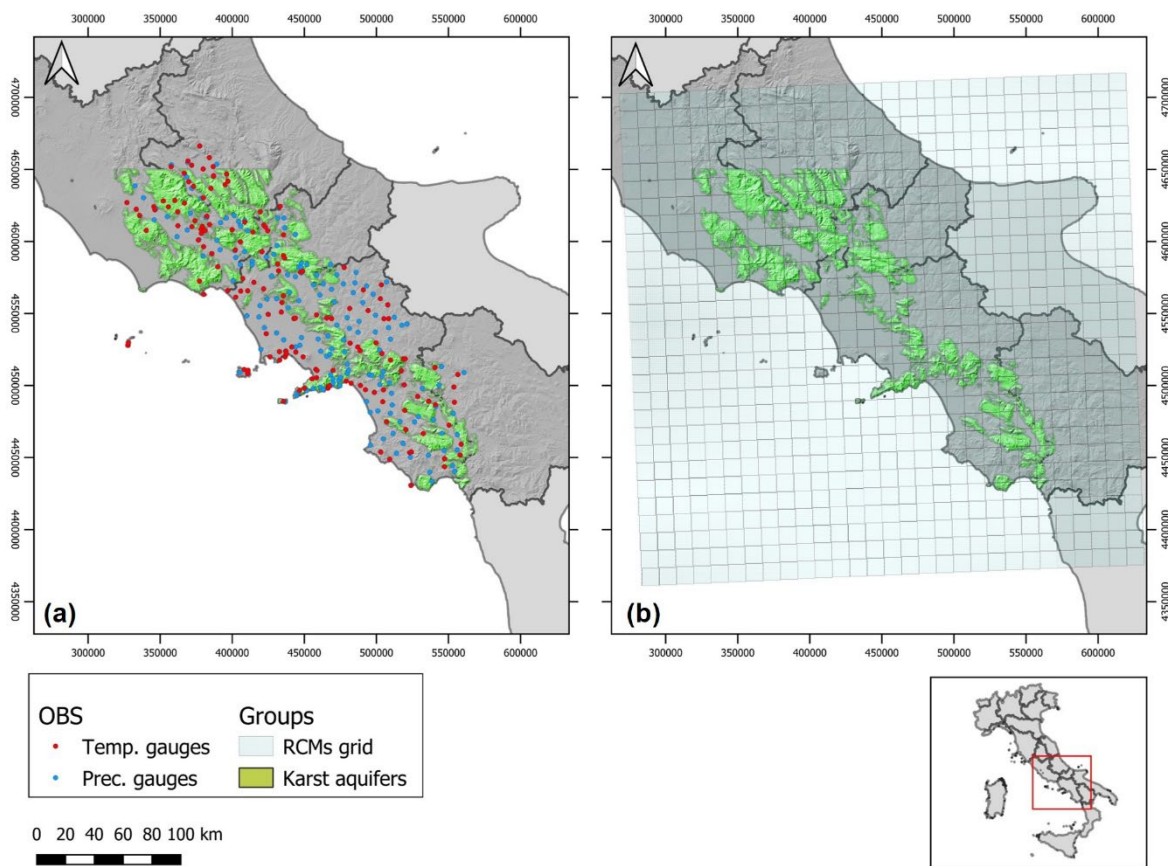
555

Figure 3: a) Map of the modelled study area showing the distributions of air temperature and rain gauge stations (OBS) which functioned, even discontinuously, in the validation period (1950-1996); b) EUR-11 RCMs grid. Karst aquifers (green colour) of the southern Apennines area also shown in both maps.

560

565

570
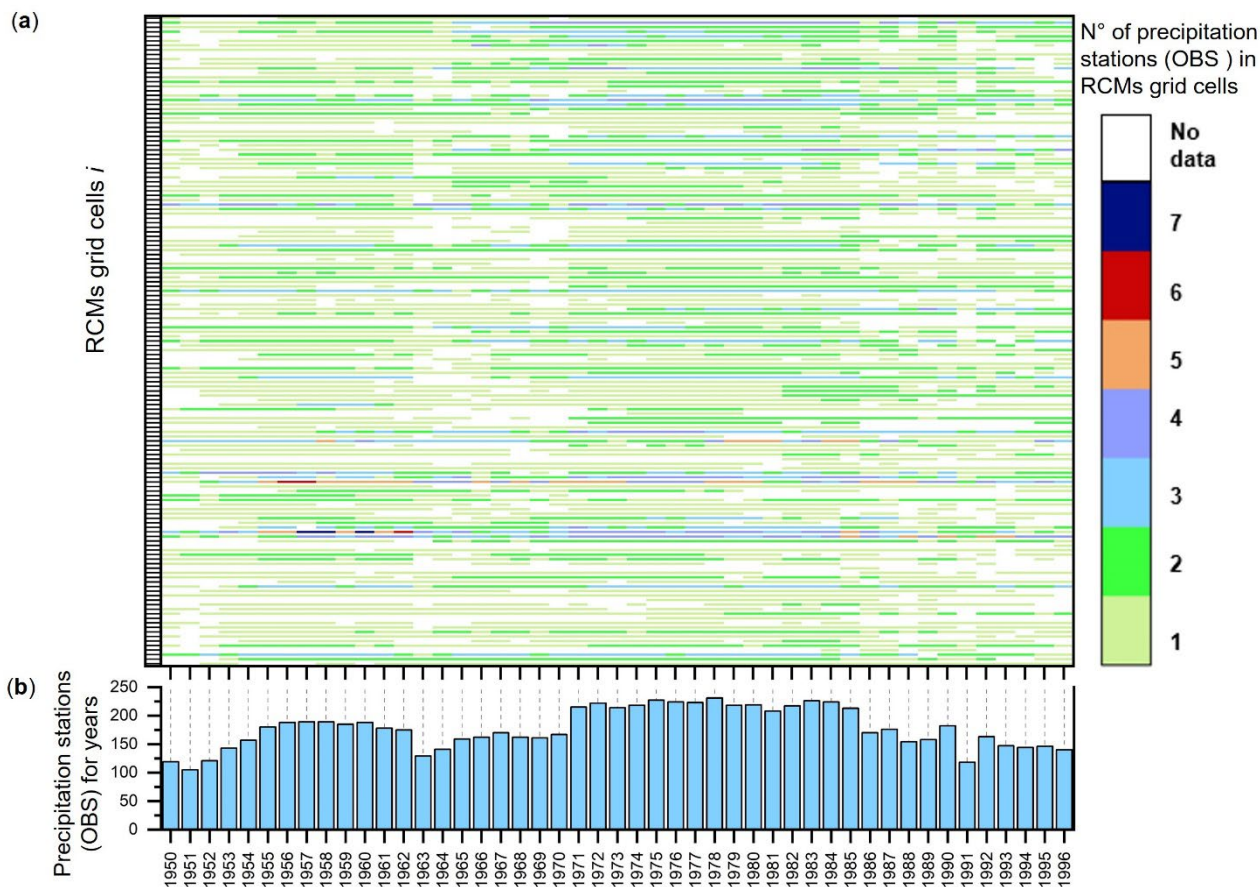
Figure 4: Spatio-temporal variation of the precipitation data across the study area: a) temporal variation of the number of precipitation stations (OBS) occurred in the validation period (1950-1996) in grid cells *i* of the RCMs; b) total number of precipitation stations (OBS) for each year.

575

580

585
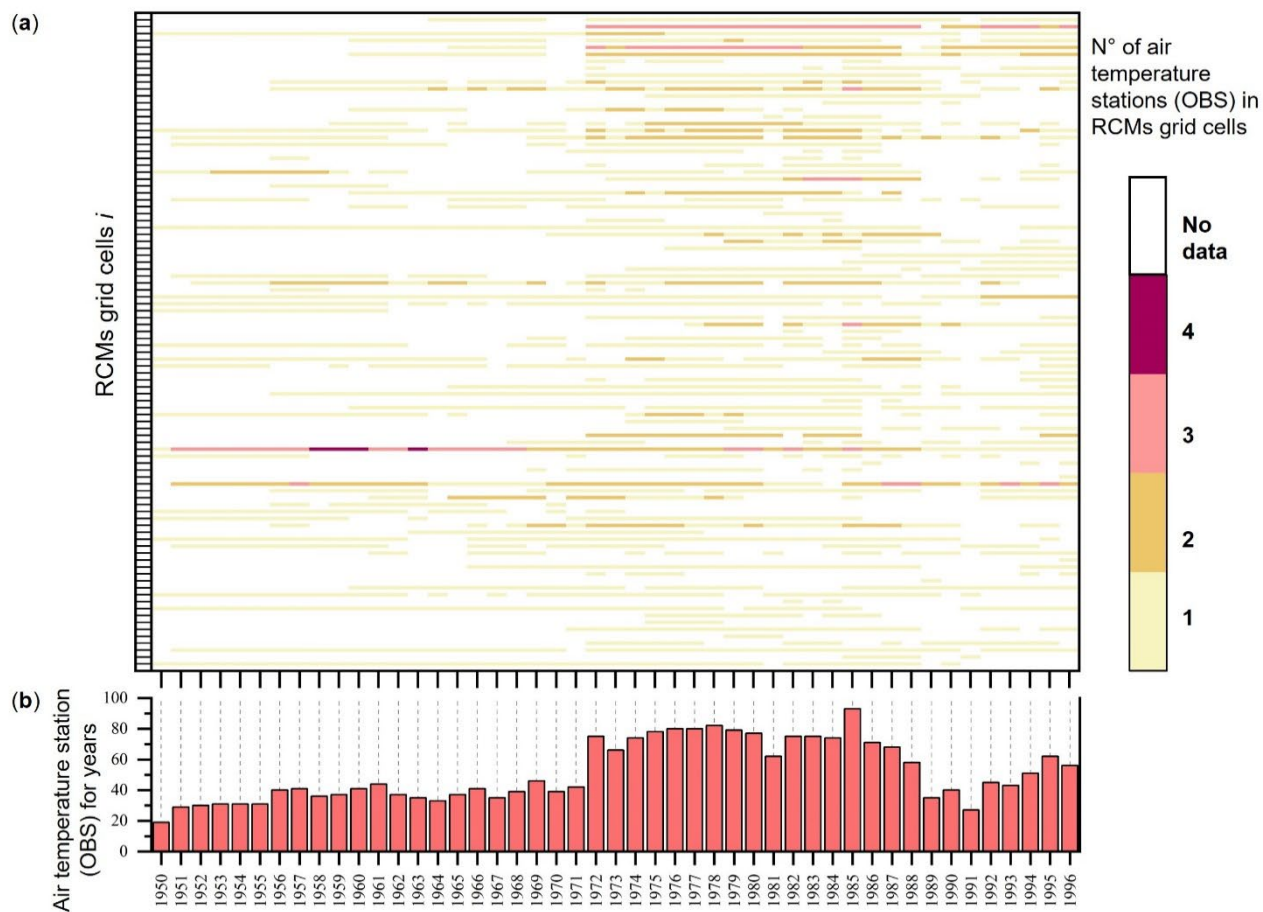
Figure 5: Spatio-temporal variation of the air temperature data: a) temporal variation of the number of air temperature stations (OBS) occurred in the validation period (1950-1996) in grid cells *i* of the RCMs; b) total number of air temperature stations (OBS) for each year.

590

595

600
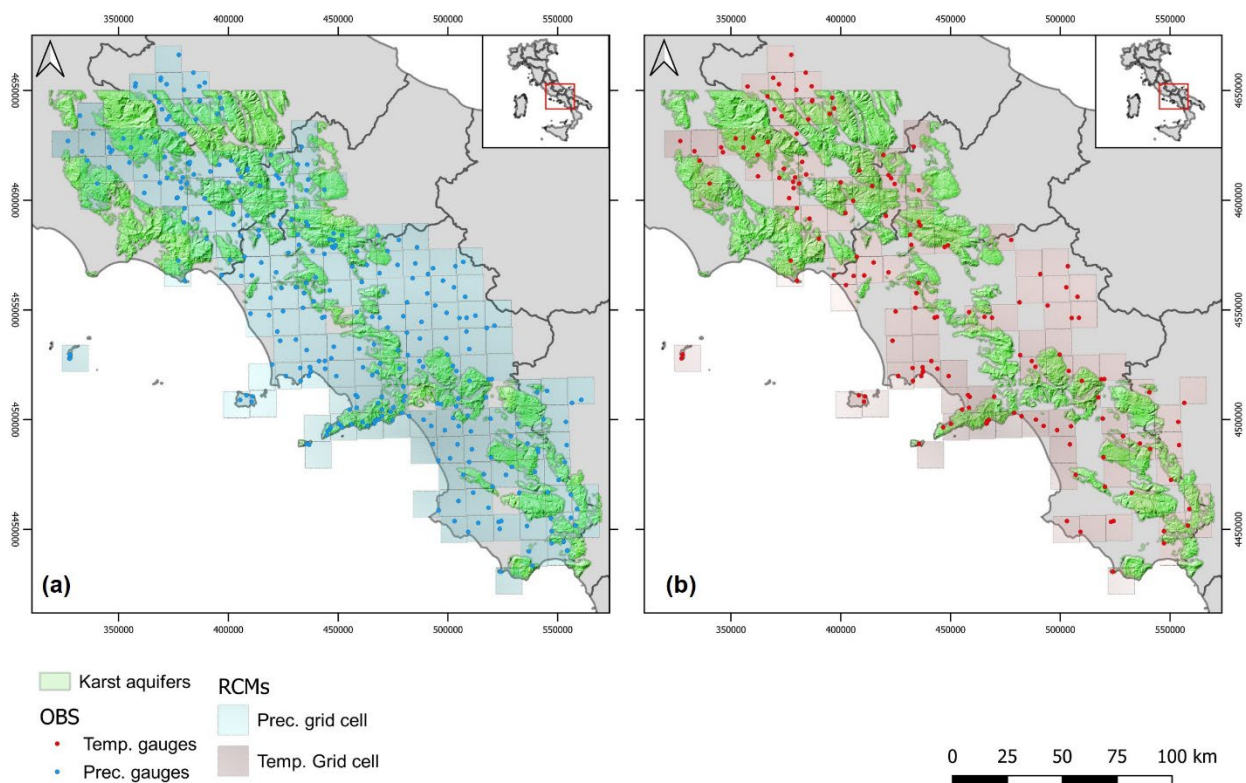
Figure 6: (a) rain gauges and (b) air temperature stations which functioned in the validation period (1950-1996) even discontinuously in space and time. The RCMs grid cells which comprised at least one monitoring station are also represented.

605

610

615
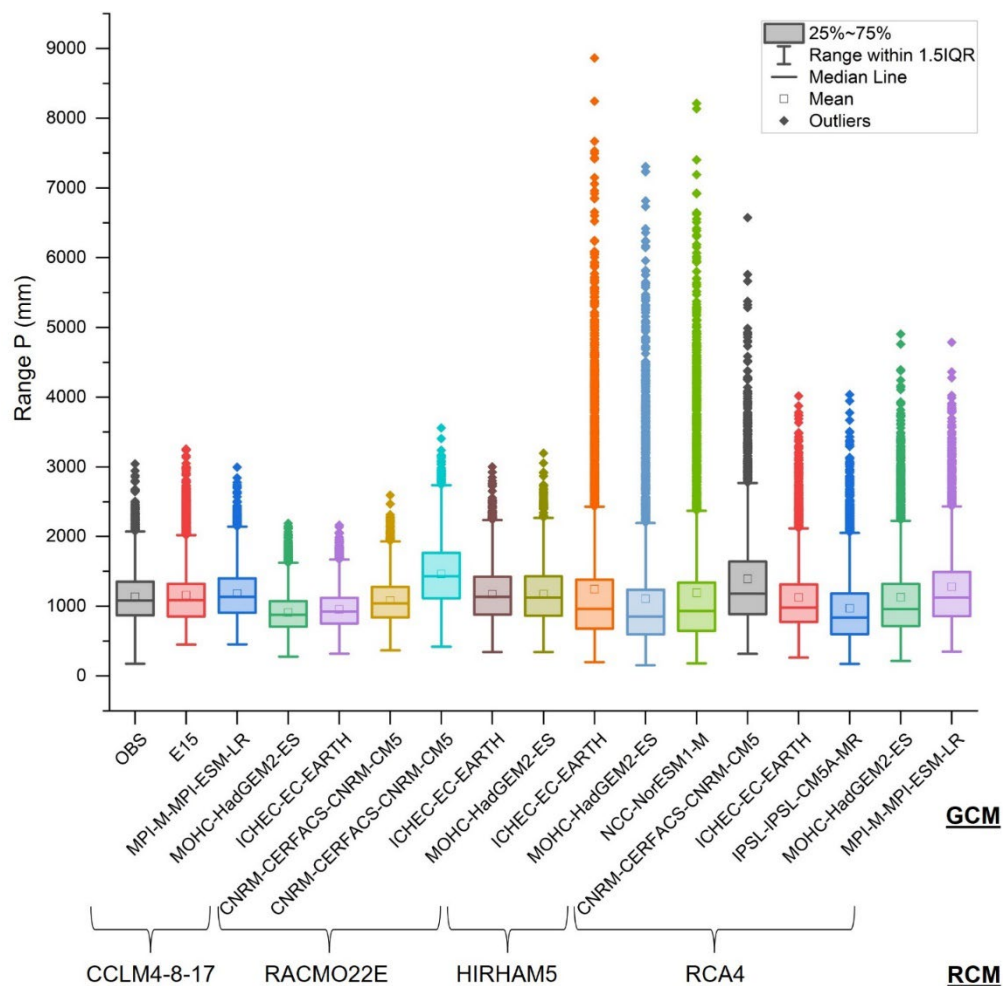
Figure 7: Box plot representing the frequency distribution of annual precipitation values of 15 RCMs considered for E15.

620

625
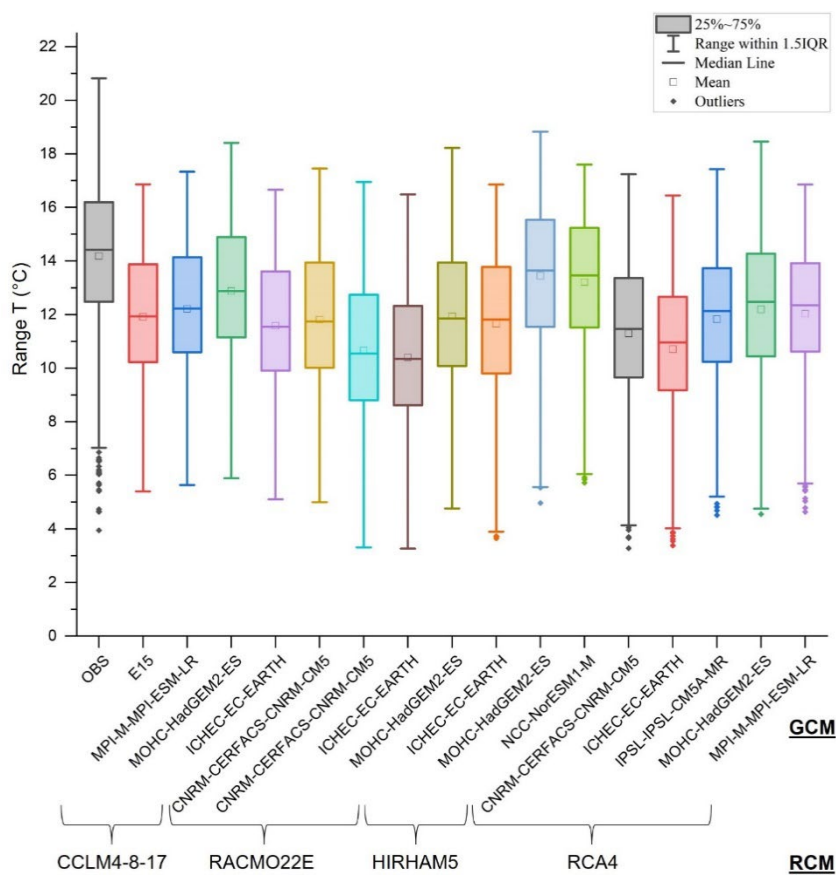
Figure 8: Box plot representing the frequency distribution of mean annual air temperature of 15 RCMs considered for E15.

630

635

640
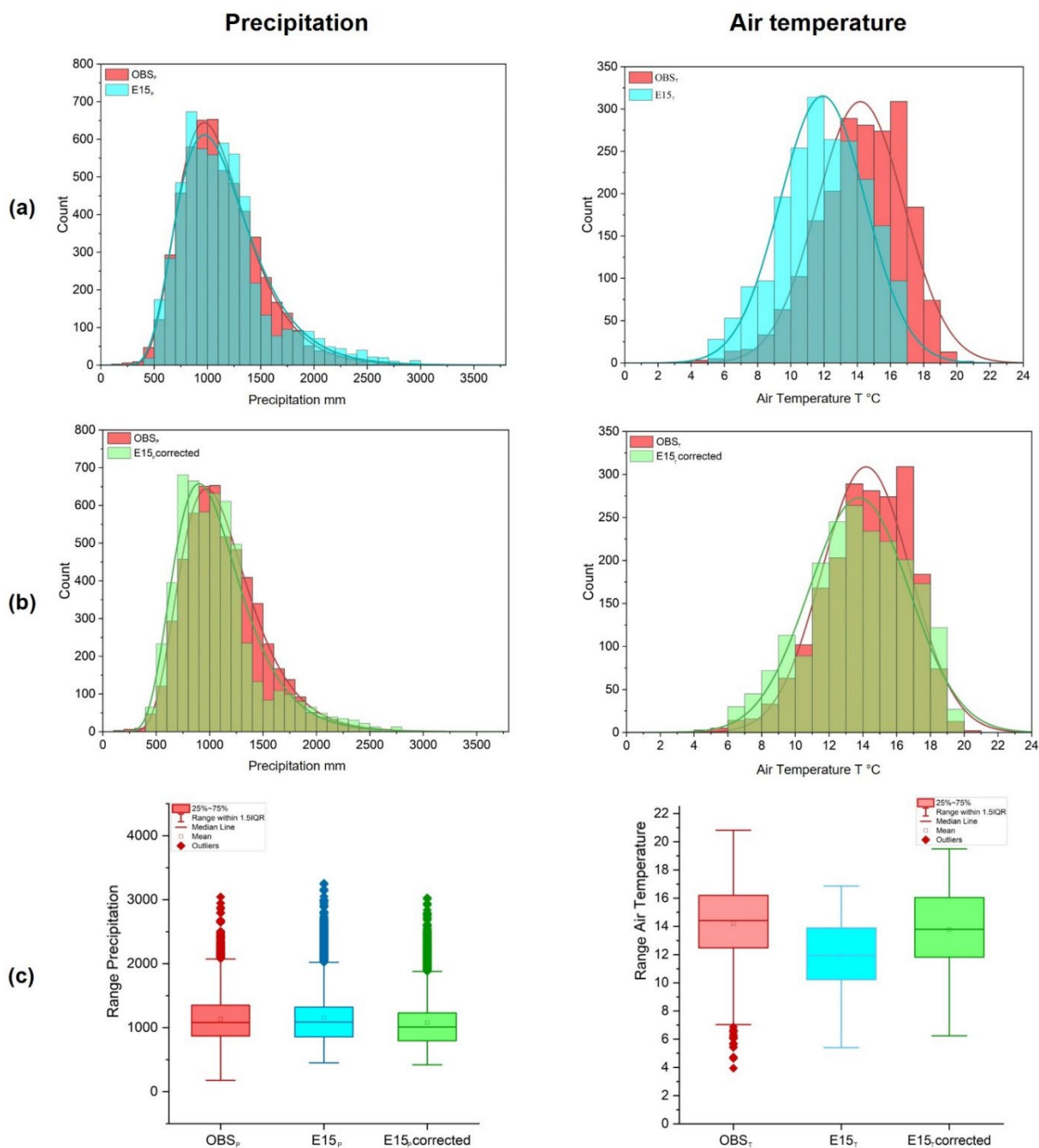
Figure 9: a) Frequency distributions of OBS$_P$ and E15$_P$ data (left) and OBS$_T$ and E15$_T$ data (right); b) frequency distributions of OBS$_P$ and E15$_P$ data (left) and OBS$_T$ and E15$_T$ data (right), after the bias correction; c) Box plot of OBS$_P$, E15$_P$ and E15$_P$ corrected data (left) and OBS$_T$, E15$_T$ and E15$_T$ corrected data (right).
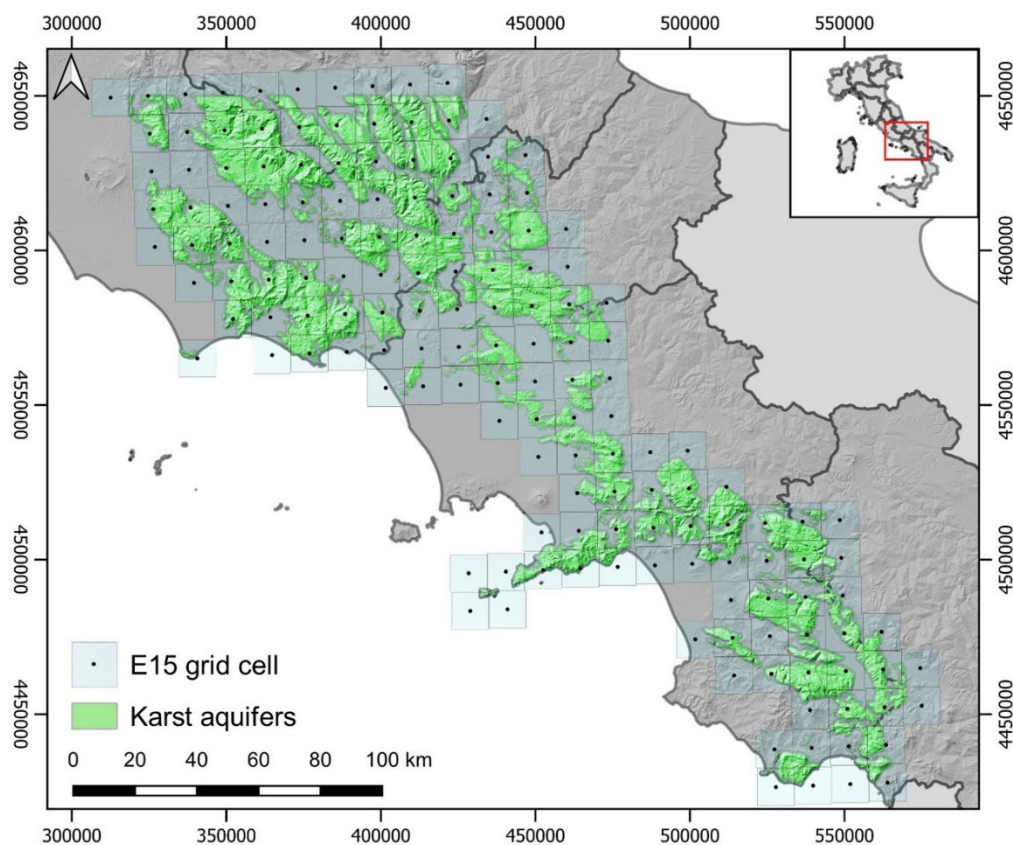
Figure 10: map of the RCMs grid cells, comprising the domain of karst aquifers. These grid cells were considered for the calculation of $E15_P$ and $E15_T$ over the karst aquifers of southern Italy for both the "historical experiment" (1950-2005) and scenario (2005-2110) periods. The centroid of each cell is showed as a small black dot.
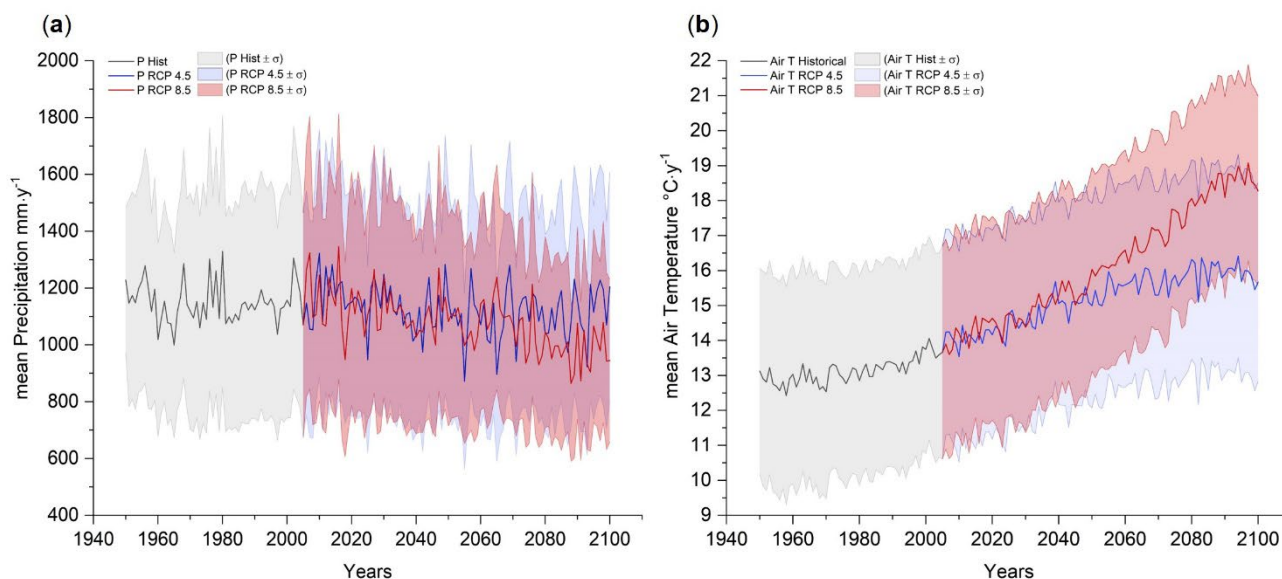
Figure 11: Time series of the "historical experiment" period (1950-2005) and scenarios (2006-2110) of RCP8.5 and RCP4.5 pathways: a) mean annual precipitation; b) mean annual air temperature. Keys to symbols: for a) and b) the confidence interval is calculated as ± σ.
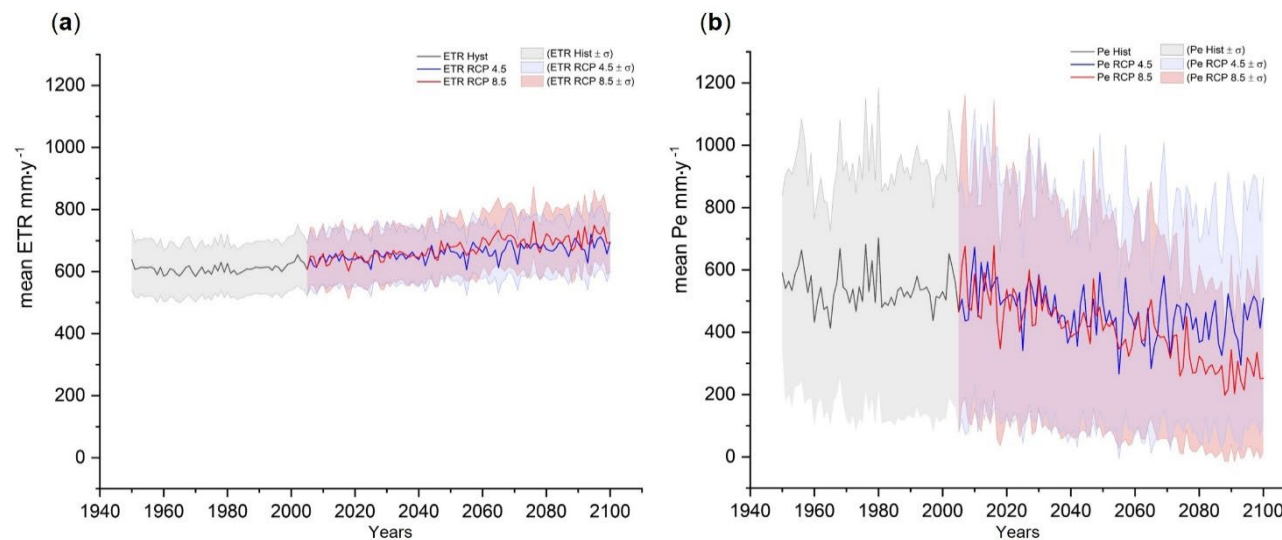
Figure 12: a) mean annual evapotranspiration ETR time series in the "historical experiment" period (1950-2005) and scenarios (2006-2110) of RCP8.5 and RCP4.5 pathways; b) mean annual effective precipitation Pe time series of the "historical experiment" period (1950-2005) and scenarios (2006-2110) of RCP8.5 and RCP4.5 pathways scenarios. Keys to symbols: for a) and b) the confidence interval is calculated as ± σ.
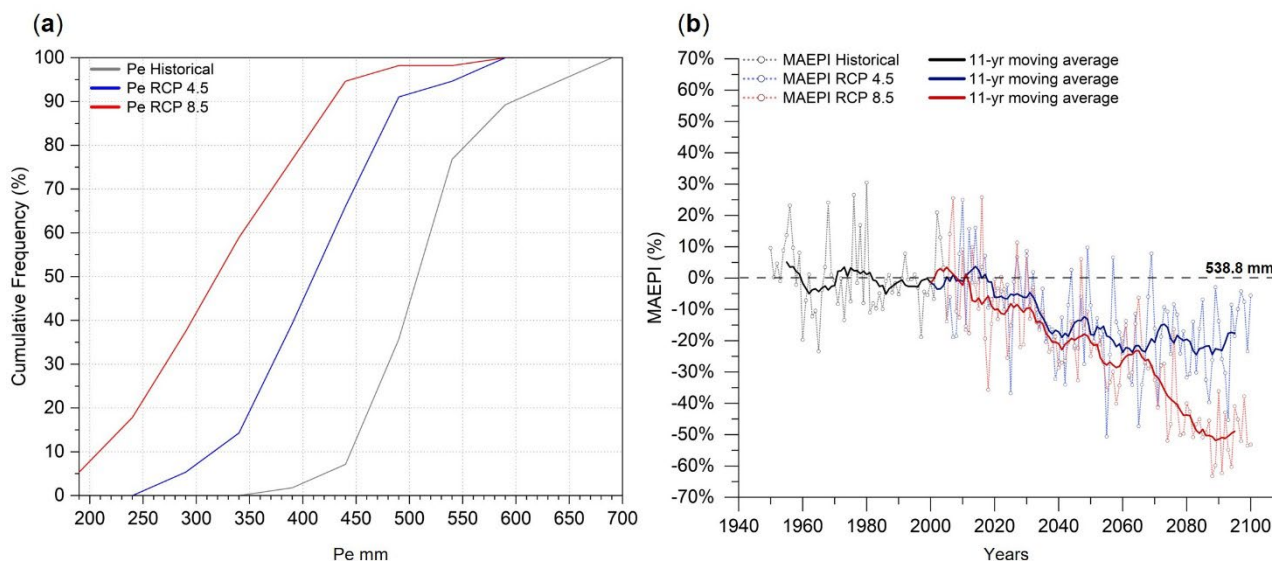
Figure 13: a) cumulative frequency of Pe time series in the "historical experiment" period (1950-2005) and scenarios (2006-2110) of RCP8.5 and RCP4.5 pathways; b) MAEPI time series of the "historical experiment" period (1950-2005) and scenarios (2006-2110) of RCP8.5 and RCP4.5 pathways scenarios. Keys to symbols: continuous thick lines represent 11-yrs moving average; dashed line and number (mm) represent the absolute effective precipitation (Pe) mean value of the historical period.

Year	Locations	GCMs/RCMs Project	N° of GCMs/RCMs	RCMs resolution km × km	Scenarios	Variables	Bias correction	Groundwater recharge quantification methods	Reference
2012	Spain	ENSEMBLES	3	25	A1b	T & P	Yes	E	Stigter et al., 2012
2014	Spain	ENSEMBLES	3	25	A1b	T & P	Yes	E	Stigter et al., 2014
2015	Spain	PRUDENCE ENSEMBLES	7	22-50	A1b A2	T & P	Yes	C	Pulido-Velazquez et al., 2015
2018	Spain	CORDEX	9	12.5	RCP8.5	T & P	Yes	E	Pulido-Velazquez et al., 2018
2019	Italy	EURO-CORDEX	13	12.5	RCP4.5 RCP8.5	T & P	Yes	N	D'Oria et al., 2019
2019	Spain	EURO-CORDEX	9	12.5	RCP8.5	T & P	Yes	E	Pardo-Igúzquiza et al., 2019
2020	Greece	EURO-CORDEX	11	12.5	RCP 2.6 RCP4.5 RCP8.5	T & P	Yes	N	Nerantzaki and Nikolaidis, 2020
2021	Greece	EURO-CORDEX	8	12.5	RCP4.5 RCP8.5	T & P	Yes	N	Voulanas et al., 2021

685 **Table 1: Literature applications of GCMs/RCMs in the framework Mediterranean areas. Key to legend: P) precipitation; T) air temperature; E) empirical; N) numerical; C) combined.**

Domain	Institution	GCM	RCM	Historical	RCP4.5	RCP8.5
EUR-11	CLMcom-BTU	MPI-ESM-LR	CCLM4-8-17	1949-2005	2006-2100	2006-2100
	CLMcom	HadGEM2-ES	CCLM4-8-17	1949-2005	2006-2099	2006-2099
		EC-EARTH	CCLM4-8-17	1949-2005	2006-2100	2006-2100
		CNRM-CM5	CCLM4-8-17	1950-2005	2006-2100	2006-2100
	KNMI	CNRM-CM5	RACMO22E	1950-2005	2006-2100	2006-2100
		EC-EARTH	RACMO22E	1950-2005	2006-2100	2006-2100
		HadGEM2-ES	RACMO22E	1950-2005	2006-2099	2006-2099
	DMI	EC-EARTH	HIRHAM5	1951-2005	2006-2100	2006-2100
		HadGEM2-ES	HIRHAM5	1951-2005	2006-2099	2006-2099
		NorESM1-M	HIRHAM5	1951-2005	2006-2100	2006-2100
	SMHI	CNRM-CM5	RCA4	1970-2005	2006-2100	2006-2100
		EC-EARTH	RCA4	1970-2005	2006-2100	2006-2100
		IPSL-CM5A-MR	RCA4	1970-2005	2006-2100	2006-2100
		HadGEM2-ES	RCA4	1970-2005	2006-2099	2006-2099
		MPI-ESM-LR	RCA4	1970-2005	2006-2100	2006-2100

690 **Table 2: EURO-CORDEX models selected and adopted in the study area to be considered for the reference ensemble (E15). EUR-11 indicate models at resolution of 0.11° (about 12.5 km).**

GCM	RCM	Reference period	Bias Precipitation			Bias Air temperature		
			Mean	Median	SD	Mean	Median	SD
MPI-ESM-LR	CCLM4-8-17	1950-1996	0.12	0.04	0.44	-0.13	-0.14	0.14
HadGEM2-ES	CCLM4-8-17	1950-1996	-0.14	-0.18	0.34	-0.08	-0.10	0.14
EC-EARTH	CCLM4-8-17	1950-1996	-0.09	-0.15	0.37	-0.18	-0.19	0.13
CNRM-CM5	CCLM4-8-17	1950-1996	0.02	-0.06	0.42	-0.16	-0.17	0.14
CNRM-CM5	RACMO22E	1950-1996	0.36	0.27	0.52	-0.25	-0.25	0.14
EC-EARTH	RACMO22E	1950-1996	0.09	0.03	0.41	-0.27	-0.27	0.14
HadGEM2-ES	RACMO22E	1950-1996	0.09	0.04	0.40	-0.16	-0.17	0.14
EC-EARTH	HIRHAM5	1951-1996	0.11	-0.10	0.83	-0.18	-0.17	0.13
HadGEM2-ES	HIRHAM5	1951-1996	-0.01	-0.19	0.74	-0.05	-0.05	0.14
NorESM1-M	HIRHAM5	1951-1996	0.07	-0.14	0.81	-0.06	-0.06	0.14
CNRM-CM5	RCA4	1970-1996	0.32	0.16	0.75	-0.19	-0.19	0.13
EC-EARTH	RCA4	1970-1996	0.08	-0.04	0.55	-0.23	-0.23	0.12
IPSL-CM5A-MR	RCA4	1970-1996	-0.08	-0.19	0.50	-0.15	-0.15	0.13
HadGEM2-ES	RCA4	1970-1996	0.05	-0.01	0.56	-0.12	-0.12	0.13
MPI-ESM-LR	RCA4	1970-1996	0.23	0.10	0.64	-0.13	-0.14	0.13

695 **Table 3: RCMs bias in comparison to the observed data (OBS) for annual total precipitation (OBS$_P$) and mean air temperature (OBS$_T$), for the validation period (1950-1996).**

	Mean precipitation (mm)				
	OBS$_P$	E15$_P$	Bias E15$_P$	E15$_P$ corr.	Bias E15$_P$ corr.
Mean	1135.4	1157.7	**0.070**	1076.6	-0.004
Standard Deviation	368.8	429.4	0.420	399.4	0.387

700 **Table 4: Mean annual precipitation of the study area, for the validation period 1950-1996 before and after the bias correction. Observed values (OBS$_P$, mm), RCM ensemble mean (E15$_P$, mm), Bias E15$_P$ (Bias E15$_P$), E15$_P$ corrected (E15$_P$ corr., mm), Bias E15$_P$ corrected (Bias E15$_P$ corr.).**

	Mean Air Temperature (°C)				
	OBS_T	$E15_T$	Bias $E15_T$	$E15_T$ corr.	Bias $E15_T$ corr.
Mean	14.19	11.92	**-0.160**	13.78	-0.024
Standard Deviation	2.63	2.57	0.120	2.970	0.143

705 **Table 5: Mean annual air temperature of the study area, for the validation period 1950-1996 before and after the bias correction. Observed values (OBS_T, °C), RCM ensemble mean ($E15_T$, °C), Bias $E15_T$ (Bias $E15_T$), $E15_T$ corrected ($E15_T$ corr, °C), Bias $E15_T$ corrected (Bias $E15_T$ corr.).**